NONINVASIVE CHEMICAL ANALYSIS BY ISOTROPIC SPECULAR REFLECTANCE SPECTROSCOPY

Walter M. Doyle
Axiom Analytical, Inc.
18103-C Sky Park South, Irvine, CA 92714

This paper describes a method of obtaining infrared absorbance spectra of bulk solids or liquids without sample preparation. It is based on the use of the Kramers-Kroenig transform to convert a first surface specular reflectance spectrum into the corresponding absorbance spectrum. The key to obtaining accurate quantitative results is an optical sampling geometry which balances the contributions from all polarization states, producing essentially isotropic data. This eliminates the polarization dependent artifacts that would otherwise result from the use of a finite range of incidence angles. The isotropic specular reflectance (ISR) approach not only allows absorbance spectra to be obtained from unmodified bulk samples but is also advantageous for analyzing thin films on reflective substrates.

INTRODUCTION

Sample preparation has been an integral part of infrared spectroscopy from the early development of the field as an adjunct to chemical qualitative analysis. As long as IR was employed primarily in the analytical laboratory, it was quite appropriate to think of sample preparation as a required step in the procedure. Solid samples, in particular, have typically been ground up and pressed into KBr pellets, crushed between diamond windows, or dissolved and recast as a thin film.

Today, IR spectroscopy is rapidly making the transition from the laboratory to the production environment, with modern FTIR systems finding increasingly routine use in on-line and near-line analysis. Here, the requirement for either continuous or repetitive measurements with little or no operator involvement make it essential that the sample preparation step be eliminated. In the case of gases and liquids, this requirement is routinely being met by the use of transmission cells and attenuated total reflecance (ATR) flow cells and probes, many of which can be operated continuously on line (ref. 1). The object of the present work was to extend these benefits of noninvasive analysis to solid samples and, in particular, to facilitate quantitative spectroscopy of intact objects — such as fabricated polymer products — without the need to grind, crush, dissolve, or otherwise destroy the item being inspected (ref. 2).

APPROACHES TO NONINVASIVE IR SAMPLING OF SOLIDS

A number of different approaches have been used for the infrared analysis of bulk solids. Several of these are quite attractive for specific types of analysis, but most of them do not exhibit the desired general applicability. Some examples are discussed in the following paragraphs.

Photoacoustic spectroscopy can analyze rough and irregular objects that are not amenable to other types of analysis (ref 3). However, this method requires rather long averaging times, is sensitive to ambient noise, and produces spectra whose characteristics can vary with measurement conditions.

Transient emission spectroscopy is attractive for the analysis of moving processes, but is not easily applied to stationary objects (ref 4).

Diffuse reflectance is widely used in the visible and near infrared regions of the spectrum where a combination of strong scattering and weak absorption renders it usable with a wide variety of samples (ref 5). However, scattering falls off rapidly with increasing wavelength. In addition, the fundamental absorptions which occur in the mid IR are orders of magnitude stronger than the overtones and combination tones typically observed in the near IR region.

As a result, diffuse reflectance has only proven useful in the mid IR when the sample is ground up and diluted in a transparent scattering matrix (ref 6). It thus does not appear to be a good candidate for noninvasive analysis.

Total hemispheric reflectance (using an integrating sphere) includes contributions from both diffuse and specular reflectance. At the long wavelengths of interest to us, it shares the deficiencies of diffuse reflectance — augmented by the lack of sufficiently high reflectance materials for coating the inside of the sphere (refs 7,8).

ATR has been used with some success for the analysis of solids. However, since ATR is a thin layer phenomenon, it is only usable if the sample surface conforms closely to the surface of the ATR element. As a practical matter, this limits the use of ATR for analysis of solids to powders and to samples which are either pliable or sufficiently flat to be positioned in intimate contact with an ATR element.

This leaves one remaining candidate: specular reflectance. Indeed, a number of workers have shown that specular reflectance data can be used to obtain absorbance spectra of a wide range of materials (refs 9,10). The general approach is to first obtain a spectrum of the specular reflectance from the first surface of the sample. This necessitates a sample which is thick enough, or sufficiently absorbing, so that no signal is obtained by reflection from the rear surface. It also requires discrimination against any observable diffuse reflectance. Once these conditions have been met, the reflectance spectrum can be converted to an absorbance spectrum by use of the Kramers-Kroenig transform, a mathematical process which relates the real and imaginary parts of a material's index of refraction (ref 11).

Previous demonstrations of the use of the Kramers-Kroenig transform to convert reflectance spectra to absorbance spectra have employed either commercial specular reflectance accessories or reflectance microscopes (refs 9,10). In each case, the need to obtain an adequate IR signal level necessitated the use of a range of reflectance angles, in some cases inclined substantially from the normal.

If we examine the mathematical relationship between specular reflectance and refractive index, we find that the form of the transform used only applies at normal incidence (ref 12). Thus, the challenge in developing a method for obtaining accurate absorbance spectra from reflectance data lies in designing a sampling system which yields a good approximation of normal incidence reflectance while providing high optical throughput. At the same time, it is desirable to maximize throughput by using a wide range of illuminating angles rather than a large illuminated area so as to minimize the requirements on sample alignment and surface flatness.

THE FUNDAMENTALS

Specular Reflectance Theory:

For this discussion, we will consider a ray of IR radiation incident on a flat surface at an angle of Go to the normal. In general, this ray will have some state of polarization. The common convention is to resolve the electric field into components parallel to and perpendicular to the plane of incidence (ie: the plane

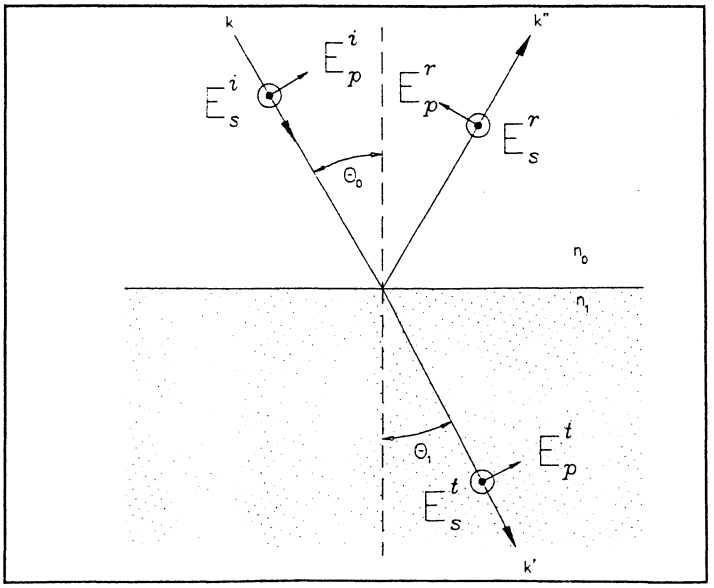

Figure 1: Specular Reflectance Ray Geometry And Electric Field Definitions - The superscripts "i", V, and "t" stand for incident, reflected, and transmitted, respectively. The subscripts "p" and "s" stand for parallel and perpendicular, respectively. The perpendicular field vectors are out of the paper.

plane containing the normal to the surface and the incident ray). These components are called Ep and E_s respectively. (Here, "p" stands for "parallel" and "s" stands for the German word "senkrecht", or perpendicular.) This geometry is illustrated in Figure 1.

In general, the relationships between the incident, reflected, and transmitted electric fields for the two polarization states are given by the Fresnel equations (ref 12). For the reflected fields these are:

$$E_s' \quad ' \quad n_0 cos8_Q \; ^{+} \; ^{\wedge}\cos 0_x$$

$$E_p^r \; _ \; _ \; n_o \cos 0_o \; - \; /^{\wedge}\cos flj$$

$$\sim E\} \; " \; ^{Tp}\sim \; n_0 cos6_Q \; _{+} \; ^{\wedge}\cos fl, \qquad (1)$$

Here E^1 and E^r are the incident and reflected fields, r_s and r_p are the amplitude reflection coefficients for the two polarization states, Go and 0i are the angles of incidence and refraction, and n_0 and ni are the indices of refraction of the two media. In most cases, the first medium will be air (n_o= 1). For the following discussion, we will assume this case and drop the subscript on ni.

At first glance, the Fresnel equations look deceptively simple. However, their use is greatly complicated by the fact that the index of refraction is a complex quantity:

$$n = n - ik$$

where the imaginary part, k, is known as the extinction coefficient. As a result, the angle of refraction and amplitude reflection coefficients are also complex, and the reflectance is given by

$$T> \quad = \; r \quad T \quad *$$
$$p,s \quad '"' \quad p,s \quad p,s$$

where indicates the complex conjugate.

The extinction coefficient is related to the absorption coefficient, *a*, by the following expression:

$$a = 4 K \nu k \qquad (2)$$

where

v is the frequency of the radiation in cm'^1.

In the general case, it is not possible to write a simple explicit expression for reflectance as a function of angle and polarization state. However, specific values can be obtained by computer solution. Typical results are shown in Figure 2 for non-absorbing media having two different refractive indices (ref 13).

At normal incidence the two polarization states are indistinguishable, and a simple expression can be written for reflectance:

$$R \; _ \; \frac{(n-1)^2 + k^2}{(n+l? \; _{+}k^2} \qquad (3)$$

It should be obvious from the above discussion that any quantitative analytical technique based on the study of specular reflectance must either make use of

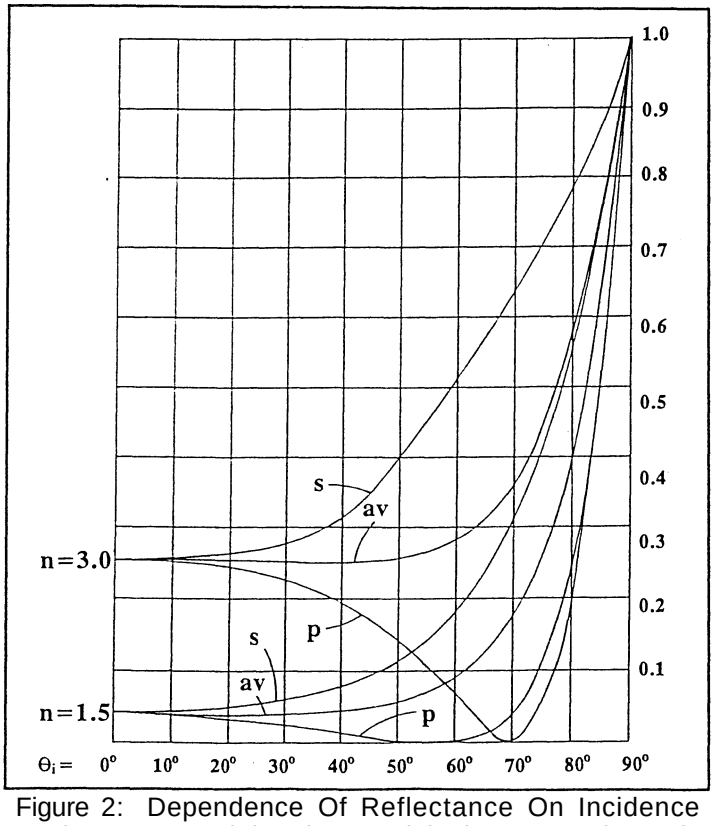

Figure 2: Dependence Of Reflectance On Incidence Angle For Two Dielectric Materials (n = 1.5 and n = 3). "s" and "p" indicate radiation polarized perpendicular to and parallel to the plane of incidence, respectively. The curves marked "av." represent the mean of the "s" and "p" values.

radiation having a well defined polarization state and angle of incidence or should operate under conditions which approximate the normal incidence condition.

The Kramers-Kroenig Transform:

The Kramers-Kroenig transform is a mathematical expression which can be used to relate the real and imaginary parts of a broad family of complex functions (ref 11). Applied to the complex refractive index, it takes the form

$$n(\nu) = n_\infty + \frac{2}{\pi} \int_0^\infty \frac{\nu' k(\nu')}{\nu'^2 - \nu^2} d\nu' \quad (4)$$

where we have explicitly shown the real and imaginary parts to be functions of the optical frequency,**.

Most FTIR manufacturers have software packages which utilize the Kramers-Kroenig transform to convert specular reflectance spectra to the equivalent absorbance spectra. In doing this, they make use of the simple relationship (Eq. 2) between extinction coefficient and absorbance as well as the normal incidence relationship (Eq. 3) for reflectance. A typical result is shown in Figure 3.

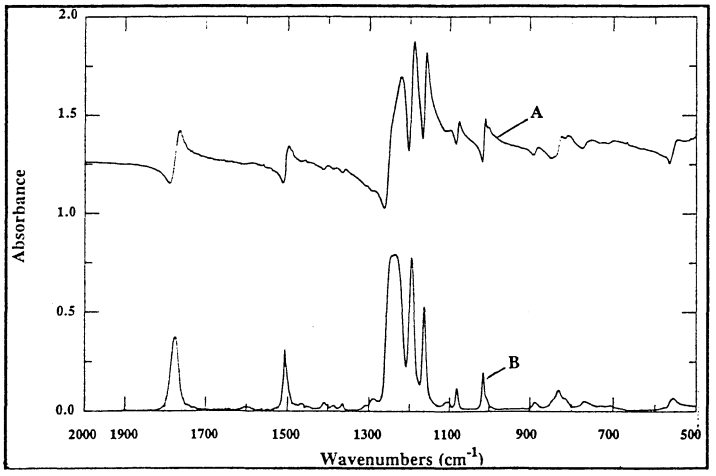

Figure 3: Trace "A" is the specular reflectance spectrum of polycarbonate (Lexan™) . Trace "B" is the absorbance spectrum obtained from "A" by using the Kramers-Kroenig transform.

THE IMPORTANCE OF NORMAL INCIDENCE OPERATION

An earlier conference paper reported on the use of computer simulation to analyze the effect of non-normal incidence on absorbance spectra computed by using the Kramers-Kroenig transform (ref 13). The procedure was as follows:

1: Starting with a reflectance spectrum of Lexan gathered at near normal incidence (similar to Figure 3) we used commercially available Kramers-Kroenig software to calculate "n" and "k" spectra. These are inherent material properties.

2: Using a custom computer program, we solved the Fresnel equations to generate "p" and "s" state reflectance spectra from the V and "k" spectra for selected angles of incidence.

3: We then used the commercial Kramers-Kroenig software to generate pseudo-absorbance spectra from the computer generated reflectance spectra.

Typical results of this exercise are given in Figures 4, 5, and 6. Reflectance spectra calculated for a 35 degree incidence angle for the two polarization states are recognizable as Lexan. However, when they are converted to pseudo-absorbance spectra, the results are quite different. And "p" state reflectance spectra calculated for high incidence angles show marked distortion.

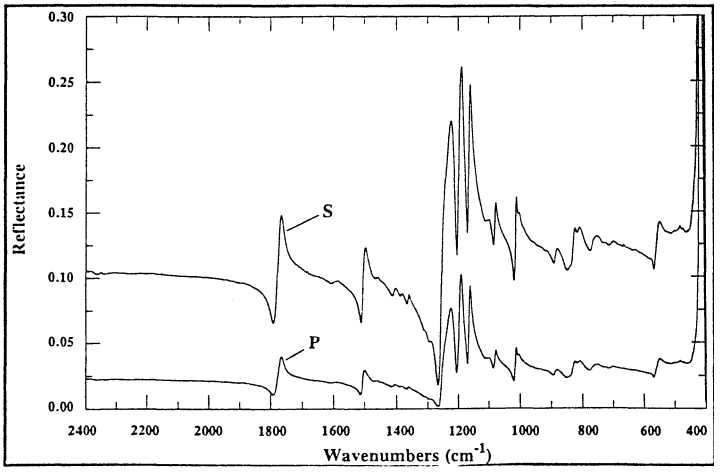

Figure 4: Computer generated reflectance spectra of Lexan for "p" and "s" state polarization at an incidence angle of 40°.

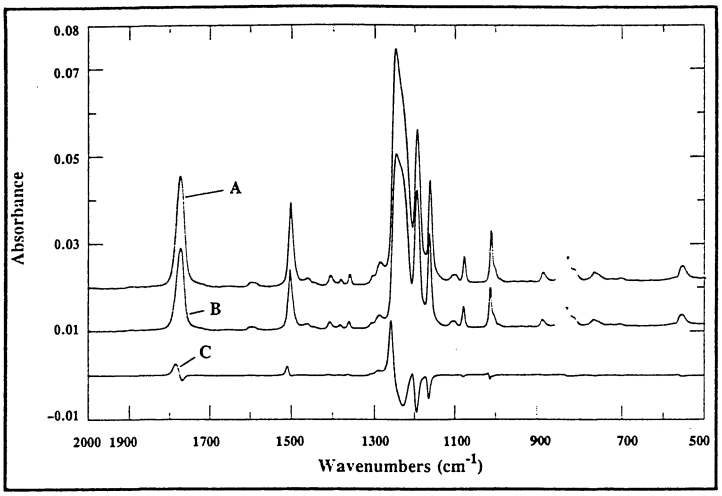

Figure 5: Traces "A" and "B" are absorbance spectra calculated from the two reflectance spectra of Figure 4. "C" is the difference between "A" and "B". Curves "A" and "B" are offset for clarity.

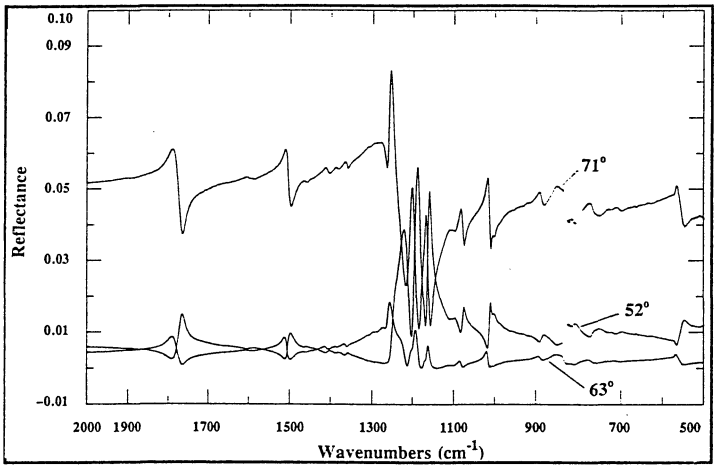

Figure 6: Computer generated reflectance spectra for "p" state polarization at three angles near Brewster's angle.

ISOTROPIC SPECULAR REFLECTANCE (ISR) SAMPLING SYSTEMS

The above example suggests that the most practical way to obtain accurate absorbance spectra from reflectance data is to collect the data under conditions which approximate normal incidence. The trick, of course, is to accomplish this while using a large collecting angle so as to maximize throughput while minimizing sensitivity to surface imperfections and sample alignment.

The key to solving this problem can be found by examining the typical angular dependence of reflectance as illustrated in Figure 2. Here we see that, even when the "p" and "s" state reflectances deviate substantially from the normal incidence value, their average remains quite independent of angle for angles as large as 40 degrees. The task is thus reduced to designing a reflectance sampling system which uses equal amounts of "p" and "s" state radiation for every angle of incidence. Once this is accomplished, the measurement will be isotropic, ie: independent of the polarization state of the incident radiation (ref 2).

The approach which we adopted employs a three bladed metallic beamsplitter, as illustrated in Figure 7 (ref 14). In this design, the beamsplitter consists of a optically flat and polished metallic plate with three electro-machined openings. Although, in the plane of the reflector, the openings are not congruent, when viewed along the direction of the incoming IR beam, they appear to be congruent 60 degree segments of a circle. This is illustrated in Figure 8. In operation, approximately 50% of the radiation passes through the openings and is focussed on the sample by a 90 degree off-axis parabolic mirror. As long as the sample is normal to the axis of the focussed beam, the reflected ray will be collected by the parabolic mirror and directed to the reflecting blade opposite the opening through which it entered. After reflection, it is focussed on the element of an IR detector.

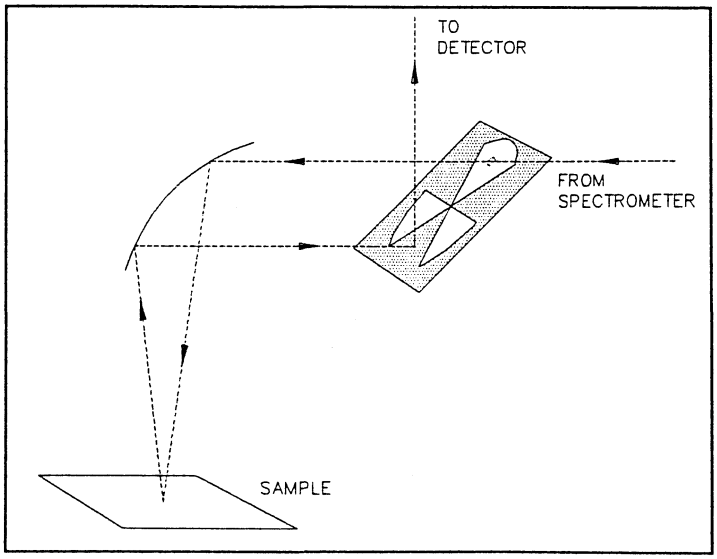

Figure 7: A sampling geometry which combines optimized round trip transmission with a good approximation of normal incidence reflectance.

The design illustrated accomplishes two things. First, as long as the beamsplitter is properly positioned relative to the focussing optics, essentially all of the radiation which passes through an opening will strike a reflecting blade on its return path. Thus, the beamsplitter can approach an overall efficiency of 50%. This is in marked contrast to a semitransparent beamsplitter which has a typical double pass efficiency of 16%. Second, the operation of the system meets our requirement calling for equal contributions from "s" and "p" state radiation for each angle of incidence. To understand this, consider Figures 8A and 8B.

First consider a ray that passes through the beamsplitter at any arbitrary location, such as the position indicated by the small circle in the upper segment of Figure 8A. Now, for any position of this ray, we can always select two other rays which bear the same relationship to the other two segments as the first ray does to its segment. These are illustrated by the circles in the lower segments.

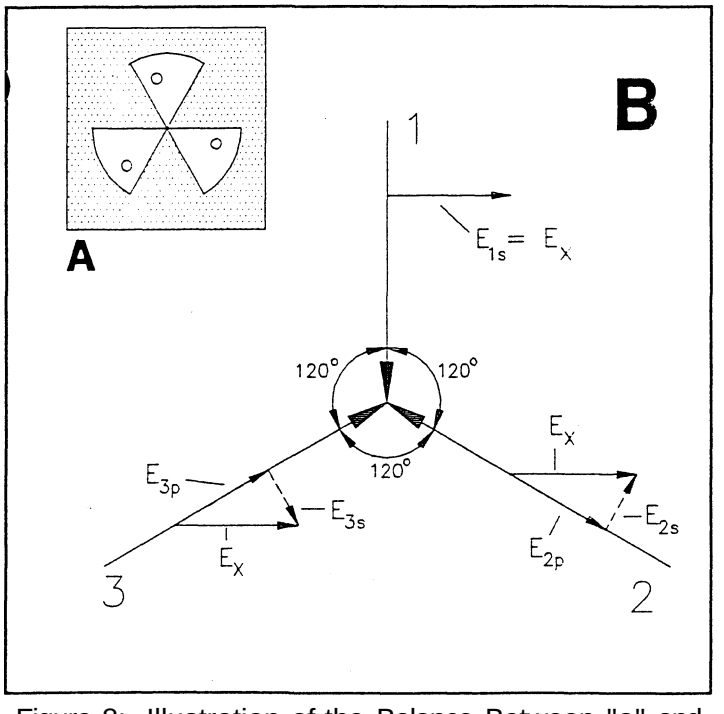

Figure 8: Illustration of the Balance Between "s" and "p" State Polarization Achieved By The Geometry illustrated In Figure 7. "8A" shows the locations of three symmetrically placed rays passing through the beamsplitter. "8B" shows the projections of these rays and their electric field vectors in the plane of the target. The field has been resolved into "s" and "p" polarization states for each ray.

We now assume that the incoming beam has a known but arbitrary state of polarization. This polarization state will be changed slightly on reflection by the focussing mirror. However, we will assume that the change is the same for each of our three rays. (This assumption is strictly true in the limit of a flat mirror.) We assume the polarization state and intensity to be the same for all three rays.

Now note that our arbitrary state of polarization can always be resolved into a pair of perpendicular Cartesian components. We will call the electric field strengths of these two components Ex and Ey respectively, with the "X" axis chosen to be perpendicular to the plane of incidence of the upper ray. We now further resolve these components into "p" and "s" state components for each ray.

In Figure 8B, the long arrows represent the projections of the incident rays on the plane of the sample. To first order in the convergence angle, the amplitudes of the "p" and "s" state polarization components will be equal to their projections in this plane. For simplicity, we will limit our discussion to this case.

Consider first the horizontally polarized component of the incoming beam, E_x. Since we have chosen our axes to make this component perpendicular to ray number 1, it is in a pure "s" state, ie:

$$E_u = E_x \quad \textit{and} \quad E_{lp} = 0$$

The situation is different for rays 2 and 3. In each case, Ex makes an angle of 30 degrees with the plane of incidence of the ray. As a result, we have

$$E_{2s} = E_{3s} = E_x \sin 30°$$

and

$$E_{2p} = E_{3p} = E_x \cos 30°$$

Now, optical intensity (ie: power density) is equal to the square of the electric field strength. Thus, the sum of the "s" state intensities for the three chosen rays will be:

$$h = \langle V^+ V^+ V \rangle$$
$$= 1.5E_X^2$$

Likewise:

$$/, - (V + EJ * EJ)$$
$$= 1.5E_X^2$$

Thus, to first order, we have achieved the desired condition of equal "s" and "p" state contributions for the "X" component of the incoming radiation.

A similar argument could be used to establish that the same balance occurs for the "y" component and thus for any arbitrary polarization state. Since the initial ray location was arbitrary, it follows that the balanced condition will occur for any combination of rays and hence for the beam as a whole.

It can be shown that the balanced condition will occur even in the presence of vignetting and to a large extent in the presence of imperfection or tilt of the sample. The three bladed beamsplitter can thus be used as the basis for a reliable system for obtaining quantitative absorbance spectra from specular reflectance data.

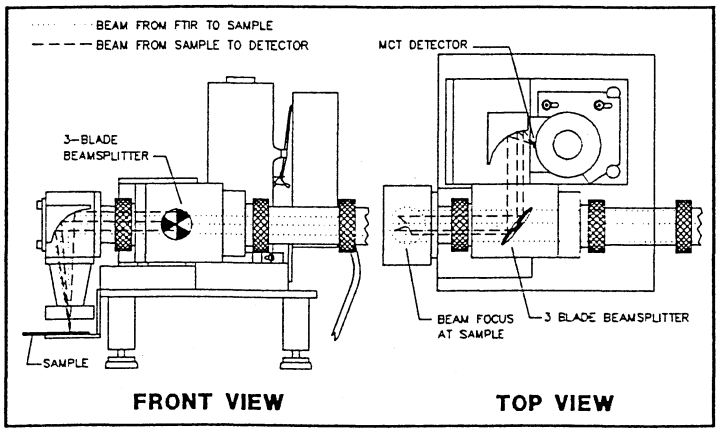

Figure 9: The isotropic specular reflectance sampling system used to obtain the data reported below (Axiom Analytical, Inc. Model SRX-332).

A PRACTICAL SURFACE SAMPLING SYSTEM BASED ON ISOTROPIC SPECULAR REFLECTANCE

Figure 9 illustrates the structure of surface sampling system employing the principles discussed above. Some of its features are outlined here.

IR radiation is transmitted from the spectrometer to the sampling system by means of a system of light guides and modular mirror assemblies (the Axiot™ system) (ref 15). In addition, a HgCdTe detector assembly is integrated into the sampling system structure. These two features allow the surface sampler to be located some distance away from the spectrometer and provide a wide degree of flexibility in positioning the system relative to a sample. If desired, telescoping Axiot sections can be used to allow the surface sampler to be scanned over the sample surface.

The optical path is enclosed and purgeable to within % inch of the sample. This allows the study of volatile liquids with minimal interference from vapor phase absorption.

The distance between the three bladed beamsplitter and the focussing parabolic mirror is set at a value which superimposes the beamsplitter and its reflected image. This minimizes vignetting, providing an overall efficiency approaching the theoretical maximum value of 50%.

The focussing mirror, and associated purge shroud and window can be rotated as a unit around the optical axis to allow either upward, forward, or downward viewing. When using the unit in the upward position, we install a thick Teflon window holder with its upper surface in the focal plane of the parabolic focussing mirror. This configuration is ideal for examining relatively small samples — which are simply placed on the Teflon holder. In the other

two positions, we use a thinner window holder which provides a ^{l}h inch offset from the sample. The forward viewing direction is usually best when viewing large objects, while the downward direction facilitates liquid analysis. Adjustable feet allow the optical axis to be adjusted for normal incidence at the horizontal liquid surface.

EXPERIMENTAL OBSERVATIONS

The data provided in this section were gathered on an Analect Model RFX-30 FTER spectrometer operating 4cm"[1] resolution. The Kramers-Kroenig software employed is Analect's fsp-6702, Version 1.0.

In obtaining the reflectance data, we first recorded a background spectrum using a gold mirror as a target. We then increased the preamplifier gain by a factor of eight to maximize the signal-to-noise ratio when recording the spectra of our samples. The reflectance spectra were then divided by the same factor to scale them properly before applying the Kramers-Kroenig transform.

A straight-forward test of the Isotropic Specular Reflectance (ISR) method is to compare its results with absorbance spectra obtained in transmission. For this test, we selected polymethylphenyl silicone (Ohio Valley Chemical Co. Type OV-17), a strongly absorbing nonvolatile oil which exhibits both sharp and broad spectral features.

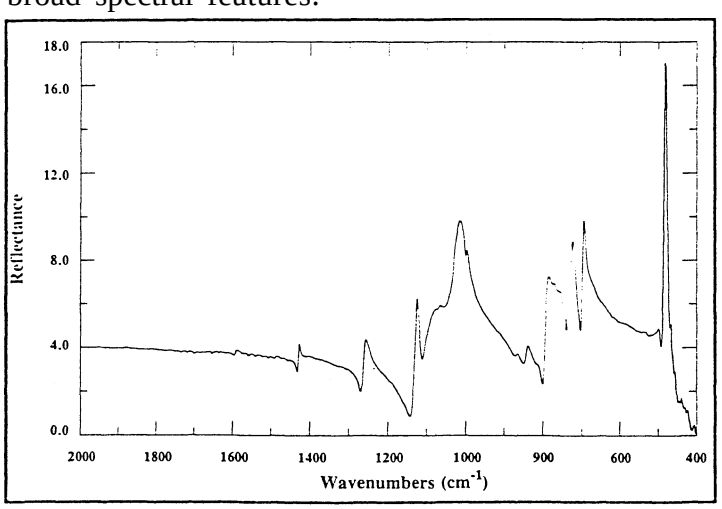

Figure 10: Specular reflectance spectrum of polymethylphenyl silicone (also known as OV-17).

To obtain the transmission data, we first tried using a conventional transmission cell with various spacers to control the sample thickness. Even with the thinnest spacer (0.025mm), the strong bands were completely saturated. We then eliminated the spacer entirely and pressed a small drop of sample firmly between two KBr plates. Even with this approach, we found that the band shapes and relative heights varied substantially from measurement to measurement. This is probably the result of nonlinearity caused by nonuniform sample thickness and the presence of microscopic air bubbles.

Figure 10 is the pure reflectance spectrum of OV-17 after dividing the raw spectrum by the appropriate factor to yield the proper scale. One additional manipulation is necessary before this data can be converted to an accurate absorbance spectrum. This is the elimination of the sharp band just below 500cm'^{l}. The reason for this is based on the fundamentals of the Kramers-Kroenig transform. The transformed spectrum is strictly correct only if the reflectance spectrum which is input extends ill the way from zero frequency to infinity. An FTIR spectrometer will typically provide data ranging from 400cm"[1] to something like 4400cm"[1]. This discrepancy is only important when there are spectral features near the limits of the spectrometer's range. Including such features in the calculation can lead to significant distortions. The solution is to simply block out such features by setting the reflectance equal to a constant value from some convenient frequency to the end of the spectrometer's range. For OV-17 (and in fact, most of the examples given below), we chose a low frequency cutoff of 550cm"[1].

The OV-17 absorbance comparison is given in Figure 11. Trace A is the absorbance spectrum calculated from reflectance data, and trace B is an absorbance spectrum obtained from the transmission measurement. Trace C is the difference between these two. Traces A and B are clearly recognizable as the same substance although there are some differences in both band heights and positions, as indicated by the non-flat difference spectrum. These are probably the result of errors in both spectra. However, it is important to note that the spectra obtained from reflectance data

were very consistent from run to run while, as noted ^bove, the transmission measurements exhibited significant variations depending on sample preparation.

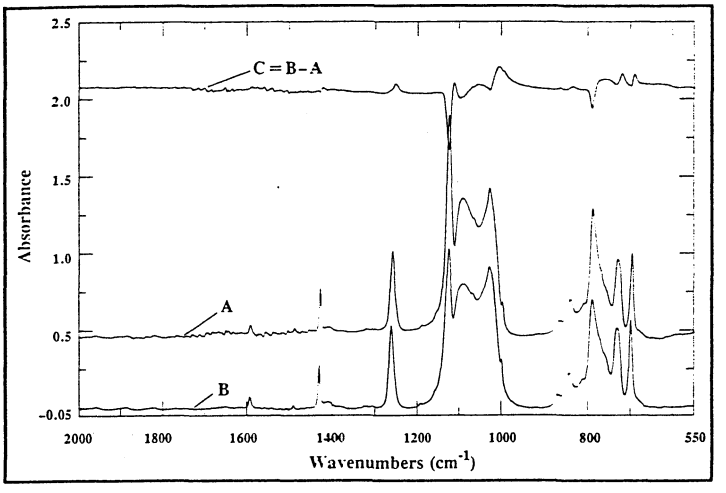

Figure 11: Comparison Of Reflectance And Transmittance Data. "A" is an absorbance spectrum of OV-17 calculated from the measured reflectance spectrum. "B" is a thin film transmission measurement of the same material. "C" is the difference between these two spectra. The features seen in the difference spectrum result from artifacts in both measurements, most notably nonlinearity of the transmission data due to sample nonconformity.

The above illustration suggests that ISR spectroscopy of bulk materials may have some important advantages over thin film transmission measurements of the same materials. This is reasonable in view of the fact that ISR is not affected by factors such as bubbles, particulate inclusions, thickness variations, index matching, and two surface interference effects that plague transmission measurements.

A further test of the utility of ISR spectra for quantitative analysis is to determine whether they give correct results for mixtures of various substances. This can be determined by subtracting the absorbance spectrum of a pure substance from the spectrum of the mixture. The remainder should be a proper spectrum of the second component. The results of such an experiment, using mixtures of alcohols, is given in Figure 12.

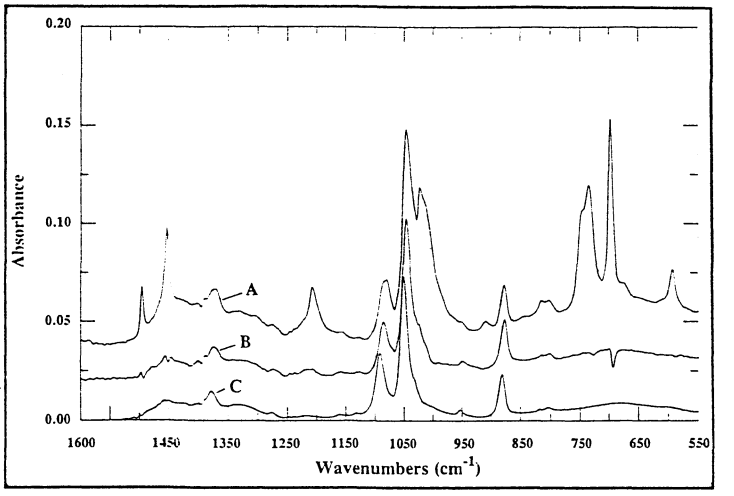

Figure 12: Example Of Absorbance Subtraction Using Reflectance Data. "A" is a mixture of 70% benzyl alcohol and 30% ethanol. "B" is the same mixture after subtracting a benzyl alcohol spectrum. "C is a spectrum of pure alcohol.

In the above illustration, liquid samples were used for the sake of experimental convenience. However, these would not represent typical applications of the technique since most liquids can be analyzed more easily by other techniques, most notably attenuated total reflectance (ATR). On the other hand, ISR may well be the method of choice for some highly reactive liquids where a non-contact technique might be especially desirable. One possible example is given in Figure 13.

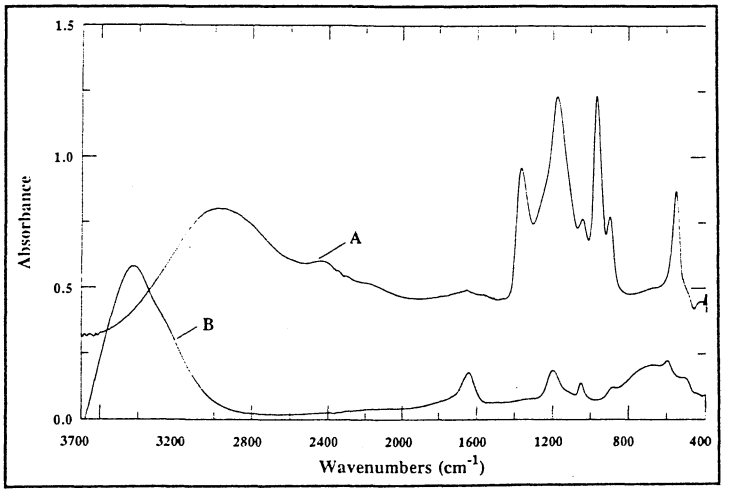

Figure 13: Spectroscopy Of Highly Reactive Substances. "A" is neat sulfuric acid. "B" is 10% sulfuric acid in water.

A more likely practical application of the use of ISR might be the inspection of a fabricated polymer product. One example of an ISR spectrum of a bulk polymer was given earlier in Figure 2. A second is given in Figure 14.

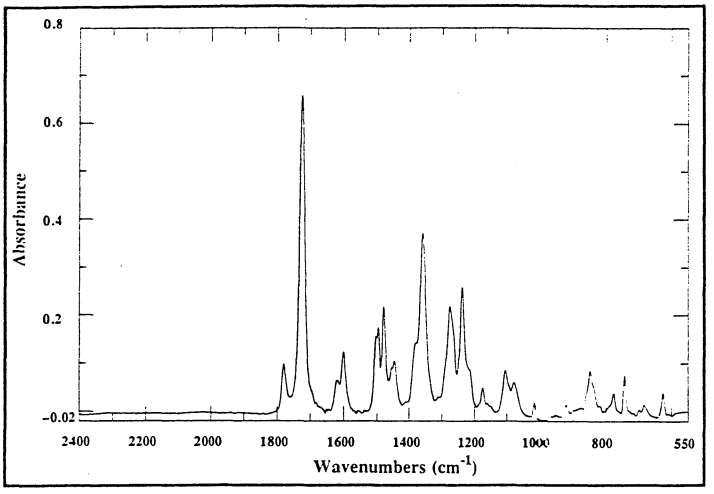

Figure 14: Absorbance spectrum of ULTEM plastic calculated from reflectance data.

The primary limitations of the ISR technique relate to the fact that it assumes that the sample surface is characterized by a single reflection. Multiple reflections can occur if the surface is rough (non-specular) or if the sample is too thin or weakly absorbing. In the latter case, some radiation will return to the sampling system after being transmitted through the sample and reflected from the rear surface or from an object behind the sample. True (internal) diffuse reflection will generally not be a factor in the mid-infrared. However, if it is significant for a given application, it may be desirable to increase the focal length of the focussing optics to discriminate against it.

SUMMARY AND CONCLUSIONS

The examples given above illustrate the utility of the isotropic specular reflectance technique for the noninvasive analysis of samples which share the following characteristics:

- Reasonable surface flatness over an area at least 4mm in diameter.
- Adequate surface smoothness so as to exhibit predominantly specular reflectance in the infrared region of the spectrum. This requires that surface imperfections are small compared to the analytical wavelengths employed.
- Either strong absorption in the spectral region of interest (characteristic of most organics) or adequate thickness so that radiation reflected from the second surface is substantially out of focus on returning to the sampling system.
- Sufficient composition homogeneity so that an analysis of the surface characteristics will provide a representative picture of the chemical structure. Obviously, this also implies that the surface of the sample must be clean.

Absorbance spectra produced from specular reflectance data by using the Kramers-Kroenig transform may exhibit distortions due to the presence of bands near the ends of the spectrometer's frequency response range. However, these spectra will generally be highly reproducible and will not exhibit the various artifacts which usually characterize thin film transmittance spectra.

An interesting characteristic of the ISR technique is the fact that, since the raw data is a direct measure of the refractive index of the sample, the spectra obtained are independent of sample thickness. Thus, any spectrum of a given material, obtained under reasonably controlled conditions, will have the same scaling. This is a useful feature for such applications as the rapid QC screening of fabricated products. For some applications, it should be possible to accelerate the analysis further by eliminating the Kramers-Kroenig transform and doing a direct comparison of the measured reflectance spectrum with a stored reflectance standard. If a significant deviation is encountered, the measured spectrum can be transformed to absorbance and the spectral subtraction technique used to identify any impurity.

In addition to its use in conjunction with the Kramers-Kroenig transform for the analysis of bulk samples, the ISR technique can be used to eliminate polarization effects in the study relatively transparent coatings on reflecting substrates. In measurements of this type (often called reflection/absorption spectroscopy), it will be necessary to account for thin film interference effects and contributions from the first surface reflectance spectrum.

REFERENCES

1. W. M. Doyle, Principles and Applications of Fourier Transform Infrared (FTIR) Process Analysis, Process Control and Quality, 2 (1992), p.50.

2. W.M. Doyle, Noncontact FTIR Spectroscopy of Bulk Solids and Liquids, in: The Pittsburgh Conference on Analytical Chemistry and Applied Spectroscopy, Chicago, IL, 1991, paper 015P.

3. P. R. Griffiths and J. A.de Haseth, Fourier Transform Infrared Spectrometry, Vol. 83, John Wiley and Sons, New York, 1986, CH. 9.

4. R. W. Jones and J. F. McClelland, Transient Infrared Transmission Spectroscopy, Analytical Chemistry, 62 (1990), p. 2247.

5. J. M. Olinger and P. R. Griffiths, Theory of Diffuse Reflectance in the NIR Region, Handbook of Near-Infrared Analysis, Marcel Dekker, New York, 1992, CH. 3.

6. P. R. Griffiths and J. A.de Haseth, Fourier Transform Infrared Spectrometry, Wiley, New York, NY, 1986, p. 194-202.

7. W. Richter, Fourier Transform Reflectance Spectrometry between 8000 cm^{-1} (1.25 /an) and 800 cm^{-1} (12.5 *fim)* Using an Integrating Sphere, Applied Spectroscopy, Vol. 37 No. 1, 1983, p.32.

8. W.G. Egan and T. Hilgeman, Integrating Spheres for Measurements Between 0.185 jnn and 12 /an, Applied Optics, Vol 14 No. 5, 1975, p.1137.

9. K. Krishnan, Applications of the Kramers-Kronig Dispersion Relations to the Analysis of FTIR Specular Reflectance Spectra, BioRad FTS/IR Notes No. 51, 1987.

10. W. Wihlborg, Applications of Reflectance FTIR Microspectroscopy, in: Spectra Tech Scan Time newsletter No. 16, 1989.

U.K. Ohta and H. Ishida, Comparison Among Several Numerical Integration Methods for Kramers-Kronig Transformation, Applied Spectroscopy, Vol. 42 No. 6, 1988, p. 952.

12. W. G. Driscoll and W. Vaughan (Ed.), Handbook of Optics, McGraw-Hill, New York, NY, 1978, p. 10-7.

13. B. Mclntosh and W. M. Doyle, Quantitative Reflectance Spectroscopy in the Mid-IR, in: The Sixteenth Annual Meeting of the Federation of Analytical Chemistry and Spectroscopy Societies, Chicago, II, 1989, paper 424.

14. W. M. Doyle, Apparatus and Method for Normal Incidence Reflectance Spectroscopy, U.S. Patent 5,015,100, May 14, 1991.

15. W. M. Doyle, Light Pipe System Having Maximum Radiation Throughput, U.S. Patent 5,054,869, Oct. 8, 1991.